**TILTED CRATER FLOORS: RECORDING THE HISTORY OF MERCURY'S LONG-WAVELENGTH DEFORMATION.** Jeffrey A. Balcerski[1], Steven A. Hauck, II[1], Peng Sun[1], Christian Klimczak[2], Paul K. Byrne[2], Andrew J. Dombard[3], Olivier S. Barnouin[4], Maria T. Zuber[5], Roger J. Phillips[6], and Sean C. Solomon[2]; [1]Department of Earth, Environmental, and Planetary Sciences, Case Western Reserve University, Cleveland, OH 44106 (jeffrey.balcerski@case.edu); [2]Department of Terrestrial Magnetism, Carnegie Institution of Washington, Washington, DC 20015; [3]Department of Earth and Environmental Sciences, University of Illinois at Chicago, Chicago, IL 60607; [4]The Johns Hopkins University Applied Physics Laboratory, Laurel, MD 20723; [5]Department of Earth, Atmospheric, and Planetary Sciences, Massachusetts Institute of Technology, Cambridge, MA 02139-4307; [6]Planetary Science Directorate, Southwest Research Institute, Boulder, CO 80302.

**Introduction:** Following MESSENGER's first flyby of Mercury in 2008, stereo photogrammetric analysis revealed areas of broad, undulating terrain in and near the Caloris basin [1]. This long-wavelength topography appeared to postdate the Caloris basin-forming event as well as subsequent plains. In addition, it was argued that the topography was not clearly the result of constructive volcanism [1]. Other possible mechanisms of formation include crustal thickening by viscous flow [2], flexural response due to asymmetric loading [3], or large-scale lithospheric folding [4].

Since the start of orbital operations in March 2011, the MESSENGER spacecraft has been returning high-resolution photographic and topographic data from its Mercury Dual Imaging System (MDIS) and Mercury Laser Altimeter (MLA) instruments. These data confirm the presence of such long-wavelength features, particularly in the Caloris region [3]. These undulations have relief between their peak and trough components of several kilometers. The "trough to trough" wavelength of these features is of order several hundred kilometers, and the features extend more than 1000 kilometers in length. When viewed from a polar stereographic perspective, it appears that they may be arranged in one or more nearly continuous bands oriented approximately circumferentially to an area near the north pole. In addition, there are more isolated areas of broad, elevated topography such as a rise situated within the northern smooth plains [3,5,6].

Mercury's craters and basins retain important clues to the relative timing and nature of surface processes. Specifically, lithospheric deformation occurring after the formation of impact craters can impose a change in attitude of nominally flat crater floors, such as those created when an impact melt sheet or subsequent volcanic fill forms a surface that follows the gravitational equipotential. Ultimately, it may be possible to constrain the timing of deformation through a combination of coarse relative age dating via assessment of crater degradation [e.g., 7] and crater size-frequency distributions on features sufficiently large to have populations dominated by primary rather than secondary craters [8,9]. Any constraints on the timing and duration of long-wavelength deformation would be important for assessing the potential causative processes.

**Approach:** We identified impact craters with substantial expanses of nominally flat floors in high-resolution MDIS images of Mercury's northern hemisphere (MLA data, used to measure accurately tilt, are dominantly restricted to the northern hemisphere due to MESSENGER's eccentric orbit with periapsis near 60–70° N). On Mercury, the transition from simple (bowl-shaped) to complex (which may have flat floors) crater morphology occurs at a diameter of ~10 km [e.g., 10]. Larger craters may possess measurable areas of relatively smooth floor. We searched MLA geoid-referenced altimetry for topographic profiles within these craters. MESSENGER's >82.5° orbital inclination means that each track has a dominantly north-south orientation except near its closest approach to the pole. By comparing MLA shot locations with crater morphology, we carefully selected data points interpreted to be representative of the crater floor. At the crater diameters of interest (> ~14 km), central peaks, rings, and wall terraces are common. Through visual inspection of multiple MDIS images with varying illumination angles, we took care to exclude such features, as well as obvious ejecta from other craters, from our measurements, using only the most pristine or innermost crater floor (in the case of multi-ringed basins). Finally, each cataloged MLA track segment was least-squares fit to a line that was then compared to the equipotential to obtain the tilt angle of the crater floor.

**Results:** Thus far, nearly 1300 MLA path segments through crater floors have been catalogued from 242 MESSENGER orbits. Of these, the vast majority are effectively horizontal, with < 200 slope measurements lying beyond one standard deviation ($\sigma$ = 0.5°) from the mean (+0.10°). A histogram of all samples (Fig. 1) illustrates the near-symmetrical, unimodal distribution of tilt magnitudes and along-track directions, with a slight northward bias indicated by the +0.10° peak offset. Because this mean is close to (but, on the basis of a *t*-test, statistically distinguishable from) zero, neglecting all samples within one standard deviation of the mean (magnitudes between -0.4º and +0.6º) results in a more pronounced mean offset of +0.40°. That is, the approximately northward tilting tail of the distribution (Fig. 1) is larger than the nearly southward tail. This asymmetry implies that in Mercury's northern hemisphere there may be a northward-tilting bias in the population of craters that have been extensively tilted. Splitting the crater population into two sets on the basis of a dividing latitude resulted in no marked change in either mean or standard deviation, indicating that there is no latitude-based dependence of either crater tilt direction or distribution of magnitudes.

Preliminary analysis indicates that there are regions where the direction of crater tilts correlates well with the slopes of the long-wavelength topography. In the Caloris area, the inclinations of the crater floors diverge from what might be considered the long axis of the elevated topography in the northern portion of the basin interior. This relationship continues to hold in the areas immediately adjacent to the basin in the east-northeast and west-southwest directions. Moreover, the craters superimposed on the broad rise on the northern smooth plains have inclined floors that dip away from the center of the feature (Fig. 2). We also note that the tilts of some sampled craters appear to be uncorrelated to the large-scale topography. These craters appear to be mainly smaller structures that may postdate the regional deformation. Conversely, they may be part of a crater population that is not located in an area substantively influenced by the long-wavelength deformation.

**Future analyses:** Here, crater tilts are measured along the MLA ground track. Thus, measured departures from the horizontal will underestimate true tilt values. In order to constrain the underestimation, it is possible to fit a plane to data within crater floors with multiple ground tracks. In these more limited cases this approach should reasonably result in a more accurate measurement of tilt magnitude and direction.

Additionally, we can obtain a misfit between the measured tilt of each crater with the local tilt, or gradient, of the long-wavelength topography at the same geographic location but projected onto the orbital track direction. Such a misfit would not necessarily represent an error, but possibly a reflection of differences in relative timing between the deformation and cratering processes or modification effects not attributable to the development of long-wavelength topography.

Further analysis of MLA data currently being collected will add to the catalog of profiled crater floors and fill in some sparsely sampled areas of the northern hemisphere. Eventually, this data set may be compared and combined with that from stereo-derived digital terrain models (DTMs) [11]. This step will be particularly helpful in Mercury's southern hemisphere, where there will be little MLA coverage and stereo DTMs will provide detailed topographic information.

**References:** [1] Oberst, J., et al. (2010) *Icarus 209*, 230. [2] Freed, A. M. (2011) personal comm. [3] Zuber, M. T., et al. (2012) *Science*, submitted. [4] Dombard, A. J., et al. (2001) *LPS 32,* abstract 2035. [5] Head, J. W., et al. (2011) *Science 333,* 1853. [6] Dickson, J. L., et al. (2012) *LPS 43*, this mtg. [7] Spudis, P. D., and J. E. Guest, (1988) in *Mercury*, Univ. Ariz. Press, 118. [8] Strom, R. G., et al. (2008) *Science 321,* 79. [9] Chapman C. R., et al. (2011) *GRL 38,* L10202. [10] Pike, R. J. (1988) Univ. Ariz. Press, 165. [11] Preusker, F., et al. (2012) *LPS, 43,* this mtg.

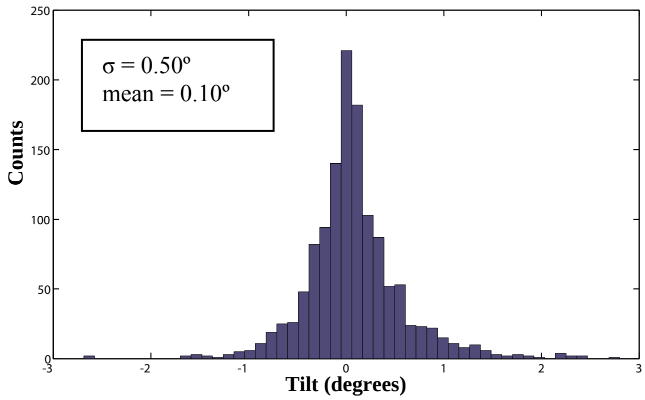


**Figure 1.** Histogram of tilt magnitude and along-track direction polarity of all measured crater floor profiles. Positive tilt direction corresponds to a northward along-track tilt.

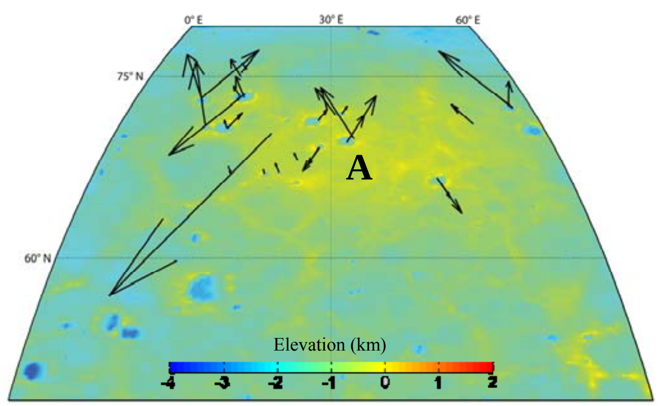


**Figure 2.** Crater floor tilts on the broad topographic rise in Mercury's northern volcanic plains, plotted over MLA gridded topography. Arrow lengths are proportional to tilt magnitudes, with the largest representing ~3º. Location **A** illustrates repeated measurements from multiple MLA tracks of a single crater, and the difference in resulting tilt directions from ascending versus descending orbital tracks.